Mechanical Properties, Morphology, and Crystal Structure of Polypropylene/Chemically Modified Attapulgite Nanocomposites

Jianjun Chen, Jinyao Chen, Shipeng Zhu, Ya Cao, Huilin Li

State Key Laboratory of Polymer Materials Engineering, Polymer Research Institute of Sichuan University, Chengdu 610065, Sichuan, People's Republic of China

Received 29 April 2010; accepted 13 October 2010
DOI 10.1002/app.33611
Published online 25 February 2011 in Wiley Online Library (wileyonlinelibrary.com).

ABSTRACT: Atactic polypropylene (aPP) was chemically grafted onto attapulgite (ATP) via the bridge linking of a polymerizable cationic surfactant and poly(octadecyl acrylate) in the presence of ultrasonic oscillation and dicumyl peroxide, and then, the modified ATP was added to a polypropylene (PP) matrix to obtain PP nanocomposites by melt blending. The results of Fourier transform infrared spectroscopy and X-ray photoelectron spectroscopy confirmed that aPP and poly(octadecyl acrylate) were chemically grafted onto ATP through a graft polymerization reaction. The results of the mechanical properties testing showed that the addition of modified ATP improved the toughness and strength of PP remarkably. The dynamic mechanical analysis indicated that the modified ATP significantly increased the storage modulus and decreased the glass-transition temperature of PP. The results of scanning electron microscopy and transmission electron microscopy showed that the modified ATP was uniformly dispersed into the PP matrix as crystal needles; this proved the presence of strong interactions between modified ATP and PP. The crystal structure analysis revealed that the β-form crystalline of PP was formed within the modified ATP. © 2011 Wiley Periodicals, Inc. J Appl Polym Sci 121: 899–908, 2011

Key words: crystal structures; nanocomposites; poly(propylene); (PP); strength; toughness

INTRODUCTION

Polypropylene (PP) is a widely used semicrystallization polymer with good processability, low cost, and relatively high mechanical properties. However, its application as an engineering thermoplastic is limited because of its poor impact resistance.[1–5] The toughness of PP could be improved with the addition of elastomer at the expense of its strength. To address these concerns, PP/clay nanocomposites have been studied for several years as a solution.[6–17] However, it is still a challenge to prepare PP/clay nanocomposites with well-exfoliated structures.

Attapulgite (ATP) is a kind of clay with the chemical formula $Mg_5(Al)Si_8O_{20}(OH)_2(OH_2)_4{\cdot}4H_2O$.[18] Despites its ribbons of 2 : 1 phyllosilicate structure, ATP differs from other layered silicates because ATP lacks continuous octahedral sheets. Within ATP, each ribbon links the next by the inversion of SiO_4 tetrahedral along a set of Si—O—Si bonds, which extend parallel to the x axis and have a width along the y axis of two linked chains. Because of this chain phyllosilicate structure, ATP can be broken easily by shear stress and forms fiber crystals.[19] Therefore, ATP has been used recently as a nanofiller to improve the properties of polymers.[20–23] Lai and coworkers[24,25] reported that purified ATP significantly improved the wear resistance of polyimide and polytetrafluoroethylene. The effect of ATP filler on the properties of nylon 6 was investigated by Subramani et al.,[26] and they found that ATP could act as an effective reinforcement for nylon 6. Some 4,4′-methylene bis(phenyl isocyanate) molecules were grafted onto the ATP surfaces through chemical bonding, and then, the modified ATP was incorporated into the polyurethane matrix through *in situ* polymerization.[20] The results showed that the tensile strength and Young's modulus of polyurethane could be increased by more than 75% when the content of the modified ATP was 10 wt %. In the study reported in ref. 23, ATP was modified with hexadecyltriphenylphosphonium bromide and 3-glycidoxypropltrimethoxysilane, and then, poly(ethylene terephthalate) (PET)/ATP nanocomposites were prepared via *in situ* polycondensation. It was found that

Correspondence to: H. Li (nic7703@scu.edu.cn).
Contract grant sponsor: National Basic Research Program of China; contract grant number: 2005CB623800.
Contract grant sponsor: Program for New Century Excellent Talents of the Ministry of Education of China; contract grant number: NCET-10-0562.

the flexural modulus of the PET/ATP composite filled with 3 wt % ATP was 41.1% higher than that of pure PET. However, ATP has attracted little attention as a nonpolar polyolefin filler, and only few studies have been devoted to composites of PP.[27,28]

In this study, with ultrasonic oscillation, ATP was broken into individual crystal needles, and then, octadecyl acrylate (ODA) was reacted with a polymerizable cationic surfactant (R303) and atactic polypropylene (aPP) on the surface of the crystal needles. Thus, a thin layer of polymer was chemically grafted onto the surface of the crystal needles, which improved the compatibility between PP and ATP. Good compatibility might have led to the uniform dispersion of ATP in the form of crystal needles and higher mechanical properties for PP. The effect of modified ATP on the mechanical properties, morphology, and crystal structure of PP were investigated as well.

EXPERIMENTAL

Materials

PP (grade F401), with a melt flow index of 2.5 g/10 min (190°C/2.16 kg), was purchased from Langang Petrochemical Co, Ltd. (Lanzhou, China). ATP clay was obtained from Anhui Mingguang Rare Minerals Co, Ltd. (Mingguang, China). ODA, xylene, and dicumyl peroxide (DCP) were all analytical grade. R303, with a molecular weight of 1100 g/mol, was provided by Henan Titaning Chemical Technology Co, Ltd. (Zhengzhou, China). The structure of R303 was as follows:

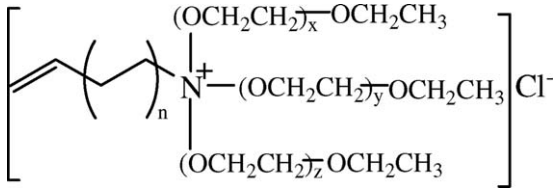

Synthesis of ODA–ATP and ODA–aPP–ATP

ODA–ATP was synthesized via polymerization with ODA as follows: 2.5 g of R303 was dissolved in 100 mL of xylene and reacted with 10 g of ATP at 30°C for 60 min. Then, 4 g of ODA and 0.12 g of DCP were added along with 400 mL of xylene into the reaction container, and the mixture was kept at 80°C for 8 h.

The ODA–aPP–ATP was synthesized as following: 2.5 g of R303 was dissolved in 100 mL of xylene and reacted with 10 g of ATP at 30°C for 60 min. Then, 20 g of aPP, 6 g of ODA, and 0.18 g of DCP were added along with 400 mL of xylene into the reaction container, and the mixture was kept at 120°C for 6 h.

The whole previous process was performed under a nitrogen atmosphere with ultrasonic oscillation. The final product was filtered and washed with xylene three times to remove the unreacted R303 and ODA. The obtained hybrid ATP was dried at 120°C *in vacuo* for 12 h.

Preparation of the PP/ATP nanocomposites

The PP/ATP nanocomposites were prepared by melt blending in a two-roll mill at 190°C with a residence time of 10 min. The clay contents were varied from 0.5 to 5 wt %. The obtained composites were molded in a platen press with 10 MPa of pressure at 190°C for 10 min and then cooled down to room temperature in another platen press with 10 MPa of pressure. Specimens about 1 and 4 mm thick were cut from the plaques for different measurements.

Fourier transform infrared (FTIR) spectroscopy

FTIR spectroscopy of ATP and modified ATP was conducted on a Tensor 27 FTIR spectrometer (Brucker, Karlsruhe, German). Scans were run at a resolution of 4 cm^{-1} from 4000 to 400 cm^{-1}. The samples were extracted by boiling in xylene for 72 h to remove the physically adsorbed R303, homopoly(octadecyl acrylate), and ungrafted aPP before scanning.

X-ray photoelectron spectroscopy (XPS)

The chemical compositions of the surfaces were determined on a Kratos XSAM 800 spectrometer (England) with an Al Kα X-ray source (1486.6 eV) at a power of 180 W (12 kV and 15 mA) and a pressure of 2×10^{-7} Pa. All of the binding energies were calibrated with the C1s peak at 284.8 eV. The samples were extracted by boiling in xylene for 72 h and a further treatment before scanning.

Mechanical properties

Tensile testing was carried out according to GB/T 1040-92 (China) on a CMT 4104 machine (Sans Material Testing Technical Co., Shenzhen, China) at a crosshead speed of 50 mm/min. The notched Izod impact strength was measured with a ZQK-20 instrument (Dahua Material Testing Technical Co., Chengde China) according to GB/T 1043-93 (China). The samples were kept at 23°C for 24 h before mechanical testing.

Dynamic mechanical analysis

The dynamic mechanical properties of PP and its nanocomposites were measured on a DMA-Q800 analyzer (TA, New Castle, American). The three-point bending mode was selected, and the measurement was carried out on a rectangular cross-sectional bar of

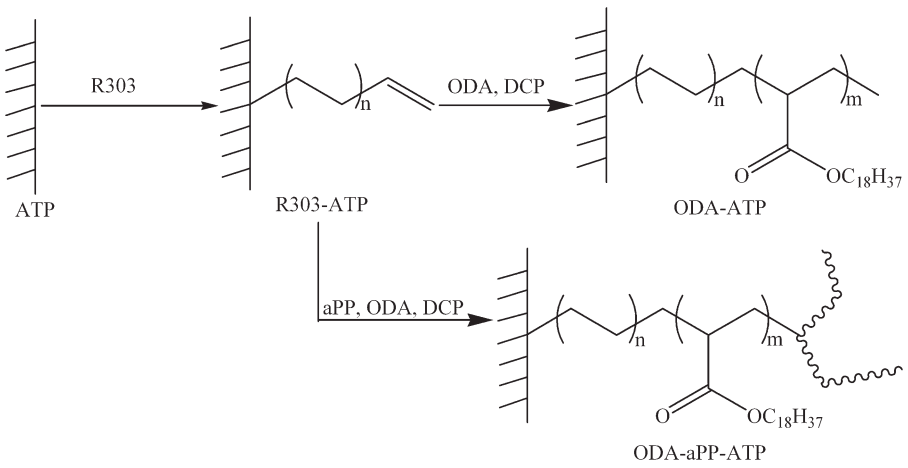

Scheme 1 Schematic representation for the reaction route for the modification of ATP.

$40 \times 10 \times 4$ mm^3 from −80 to 160°C at a heating rate of 5°C/min and a frequency of 5 Hz.

Morphological characterization

Scanning electron microscopy (SEM)

The impact fracture surface morphologies of the PP/ATP nanocomposites were observed with a Philip SEM instrument (Amsterdam, Netherlands) with an accelerating voltage of 20 kV. The surface was coated with a thin layer of gold to reduce charge buildup on the surface and to improve the conductivity.

Transmission electron microscopy (TEM)

TEM observations were carried out with an H-7100 instrument (Hitachi, Tokyo, Japan) with an accelerating voltage of 100 kV. The ultrathin samples were microtomed at 20°C by a Reichert Ultracut cryoultramicrotome (vienna, Austria) without staining.

Wide-angle X-ray diffraction (WAXD)

The crystal structures of PP and its nanocomposites were assessed through WAXD experiments at room temperature with a Philip X' Pert Pro diffractometer; the X-ray beam was nickel-filtered Cu Kα [wavelength (λ) = 0.1542 nm] radiation, and the diffractometer was operated at an acceleration voltage of 40 kV and with a current of 35 mA. The corresponding data were collected from 5 to 40° at a scanning rate of 6°/min.

Differential scanning calorimetry

The melting behaviors of PP and its nanocomposites were determined under a constant nitrogen flow on a Mettler Toledo DSC 1 differential scanning calorimeter thermal analyzer (Zurich, Switzerland). Approximately 6 mg of each sample was placed in a standard aluminum crucible and heated from room temperature to 200°C at a heating rate of 10°C/min.

RESULTS AND DISCUSSION

Surface modification of ATP

The cation in ATP can be exchanged with a cationic surfactant.[29,30] Therefore, R303, which possesses active end-functional groups (—CH=CH$_2$), was first used to ionically exchange with ATP. The content of R303 was 10.3 wt %, as measured by thermogravimetric analysis. The R303 chemically grafted onto ATP could copolymerize with ODA in the presence of an initiator, and the obtained ATP was denoted as ODA–ATP. When DCP was used as the initiator, the two free-radical species induced by the thermal decomposition of DCP was able to abstract hydrogen atoms from aPP chains and add to the double bonds of ODA.[31,32] At the same time, the free radicals arising from ODA might have coupled with those coming from R303 exchanged into ATP. In this way, aPP was chemically grafted onto R303–ATP through the polymerization of ODA and another modified ATP (ODA–aPP–ATP) was obtained. The grafting reaction route is shown in Scheme 1. To verify this reaction, FTIR and XPS measurements were performed.

The FTIR spectra of the original ATP and modified ATP are shown in Figure 1. New absorption bands at 2971, 2927, and 1356 cm^{-1}, which corresponded to the stretching of —CH$_3$, —CH$_2$, and C—O—C, respectively, were observed in the FTIR spectra of R303–ATP. It is clear that R303 was grafted chemically onto ATP through a cationic-exchange reaction. Compared with R303–ATP, the new absorption bands at 1734 cm^{-1}, which corresponded to the stretching of C=O in poly(octadecyl

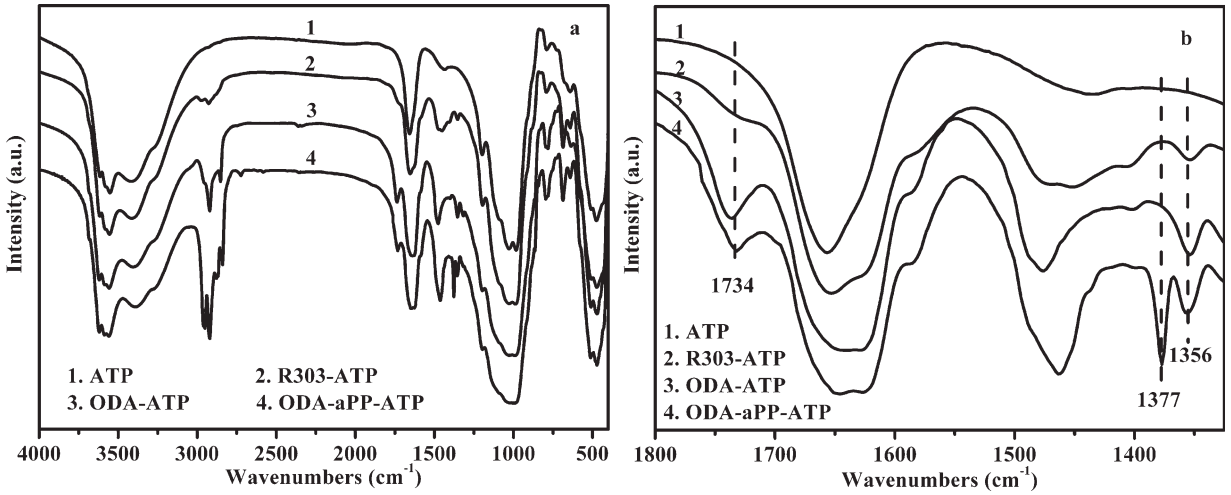

Figure 1 FTIR spectra of original ATP and modified ATP: (a) survey spectra and (b) spectra from 1800 to 1300 cm^{-1}.

acrylate), appeared in the FTIR spectra of ODA–ATP. This indicated that poly(octadecyl acrylate) was chemically grafted onto ATP through copolymerization with the R303 exchanged into ATP. The new absorption bands at 1734 and 1377 cm^{-1}, which were attributed to the stretching of C=O in poly(octadecyl acrylate) and the bending of $-CH_3$ in aPP, respectively, were observed in the FTIR spectra of ODA–aPP–ATP; this result suggested that aPP was chemically grafted onto ATP through the bridge linking of R303 and poly(octadecyl acrylate).

The chemical compositions on the surfaces of original ATP and modified ATP derived from XPS spectra (Fig. 2) are listed in Table I. The addition of R303 introduced a considerable amount of carbon onto the surface of ATP, and the C/Si ratio increased markedly when ATP was modified with R303, which proved that R303 was chemically grafted onto ATP.

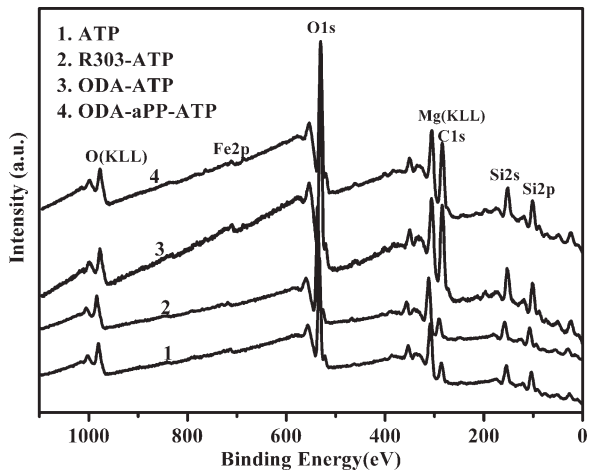

Figure 2 XPS survey spectra of raw ATP and modified ATP. The "KLL" is the Auger electron which was excited in the XPS test.

The content of carbon on the surface of ODA–ATP was further increased to 34.71%, which confirmed that ODA was grafted onto ATP chemically by copolymerization with the R303 exchanged into ATP. The carbon content and C/Si ratio on the surface of ODA–aPP–ATP were higher than those of R303–ATP. We suggest that aPP was chemically grated onto ATP through the bridge linking of R303 and poly(octadecyl acrylate). These results were consistent with those of FTIR spectroscopy.

Mechanical properties of PP and its nanocomposites

The mechanical properties of PP and its nanocomposites are listed in Table II. As shown in Table II, the impact strength and tensile strength of PP changed slightly with the addition of the original ATP. However, the impact strength and tensile strength of PP increased significantly with the addition of either ODA–ATP or ODA–aPP–ATP. Moreover, the impact strength and tensile strength of the PP/ODA–aPP–ATP nanocomposites were higher than those of PP/ODA–ATP nanocomposites with the same content of filler. With the addition of 3 wt % ODA–aPP–ATP, the impact strength and tensile strength of PP increased by 123 and 23%, respectively, over those of pure PP. These results were attributed to the

TABLE I
Surface Compositions (atom %) of the Original ATP and the Chemically Modified ATP

Sample	C (%)	O (%)	Si (%)	Al (%)	Mg (%)	Fe (%)	C/Si
ATP	20.82	53.80	14.64	4.58	4.78	1.38	1.42
R303–ATP	25.87	50.84	12.93	3.65	5.56	1.15	2.00
ODA–ATP	34.71	44.02	12.84	3.60	4.83	1.00	2.70
ODA–aPP–ATP	39.85	42.81	10.63	1.88	3.84	0.98	3.75

TABLE II
Mechanical Properties of PP and Its Nanocomposites

Sample	phr	Izod impact strength (kJ/m^2)	Yield strength (MPa)	Tensile strength (MPa)	Young's modulus (MPa)	Elongation at break (%)
PP		3.58	32.00	32.00	833	123.1
PP/ATP	0.5	3.67	32.20	32.20	936	129.4
	1	3.82	32.60	32.60	1137	96.8
	2	3.69	32.80	32.80	1645	83.9
	3	3.57	32.90	32.90	1140	80.5
	5	3.23	32.70	32.70	1099	66.2
PP/ODA–ATP	0.5	4.91	35.51	35.51	1131	101.1
	1	5.54	36.27	36.27	1332	105.4
	2	5.32	36.98	36.98	1759	78.8
	3	5.11	35.84	35.84	1378	92.8
	5	4.85	35.07	35.07	841	88.6
PP/ODA–aPP–ATP	0.5	6.99	37.00	37.00	1301	107.1
	1	7.46	37.50	37.50	1748	125.8
	2	7.57	38.50	38.50	3307	134.8
	3	8.01	39.40	39.40	2149	150.9
	5	7.20	37.50	37.50	1981	115.1

good compatibility between ATP and the PP matrix, which was enhanced by the chemical modification of ATP. In addition, all of the nanocomposites showed higher moduli compared with pure PP. However, the improvement over PP/modified ATP was larger than that of PP/ATP. These results suggest that the chemical modification was essential for achieving higher mechanical properties for PP.

Dynamic mechanical properties of PP and its nanocomposites

To confirm the assumption that the reinforcement effect was due to the well-dispersed clays in the PP nanocomposites, the dynamic modulus of PP and its nanocomposites were plotted versus temperature (Fig. 3). As shown in Figure 3(a), the storage moduli of the nanocomposites were all higher than that of pure PP, which indicated that ATP could act as an effective reinforcement material for PP. However, compared with the PP/original ATP composites, the storage moduli of the PP/modified ATP nanocomposites decreased slightly. This might have been due to the plasticization effect caused by the molecules at the interface between the filler and the matrix.

Figure 3(b) shows the curves of the loss moduli of PP and its nanocomposites versus temperature. The maximum heat dissipation occurred at the temperature where the loss modulus was maximum, which corresponded to the glass-transition temperature (T_g) of the system.[33] The T_g values derived from the curves of the loss modulus versus temperature are listed in Table III. The introduction of original ATP resulted in a slight increase in T_g of the PP matrix; this might have been due to the fact that the mobility of the PP molecular chain was limited by original

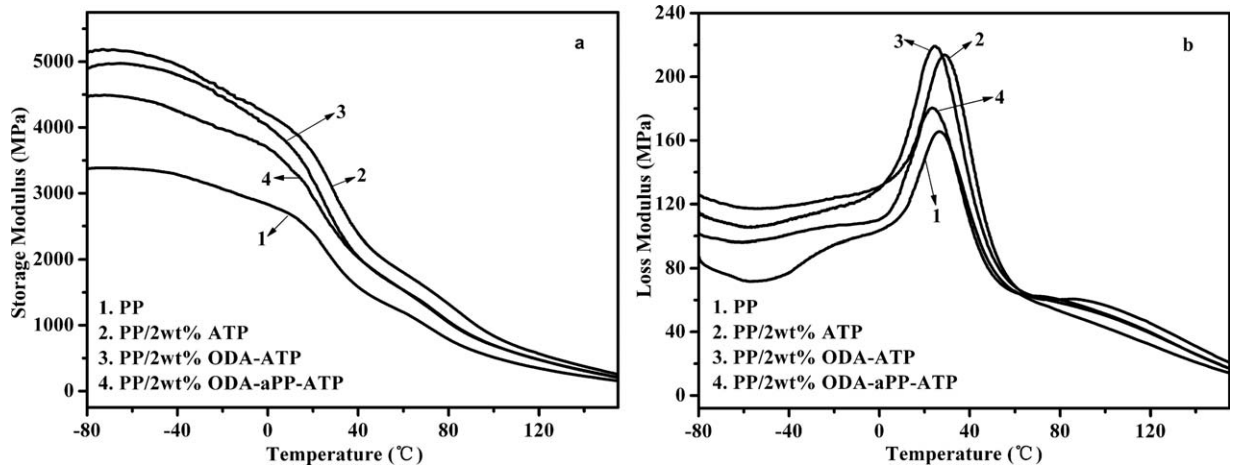

Figure 3 Dynamic mechanical properties of PP and its nanocomposites: (a) storage modulus and (b) loss modulus.

TABLE III
T_g Values of PP and Its Nanocomposites

	Sample			
	PP	PP/2 wt % ATP	PP/2 wt % ODA–ATP	PP/2 wt % ODA–aPP–ATP
T_g (°C)	26.6	28.6	24.8	23.2

ATP.[20] However, for the PP/modified ATP nanocomposites, the mobility of the PP molecular chain was promoted by the modifier at the interface; this led to a slight decrease in T_g of the nanocomposites.

Morphologies of the PP/ATP nanocomposites

The morphology of a polymer composite plays a very important role in its physicomechanical properties.[34]

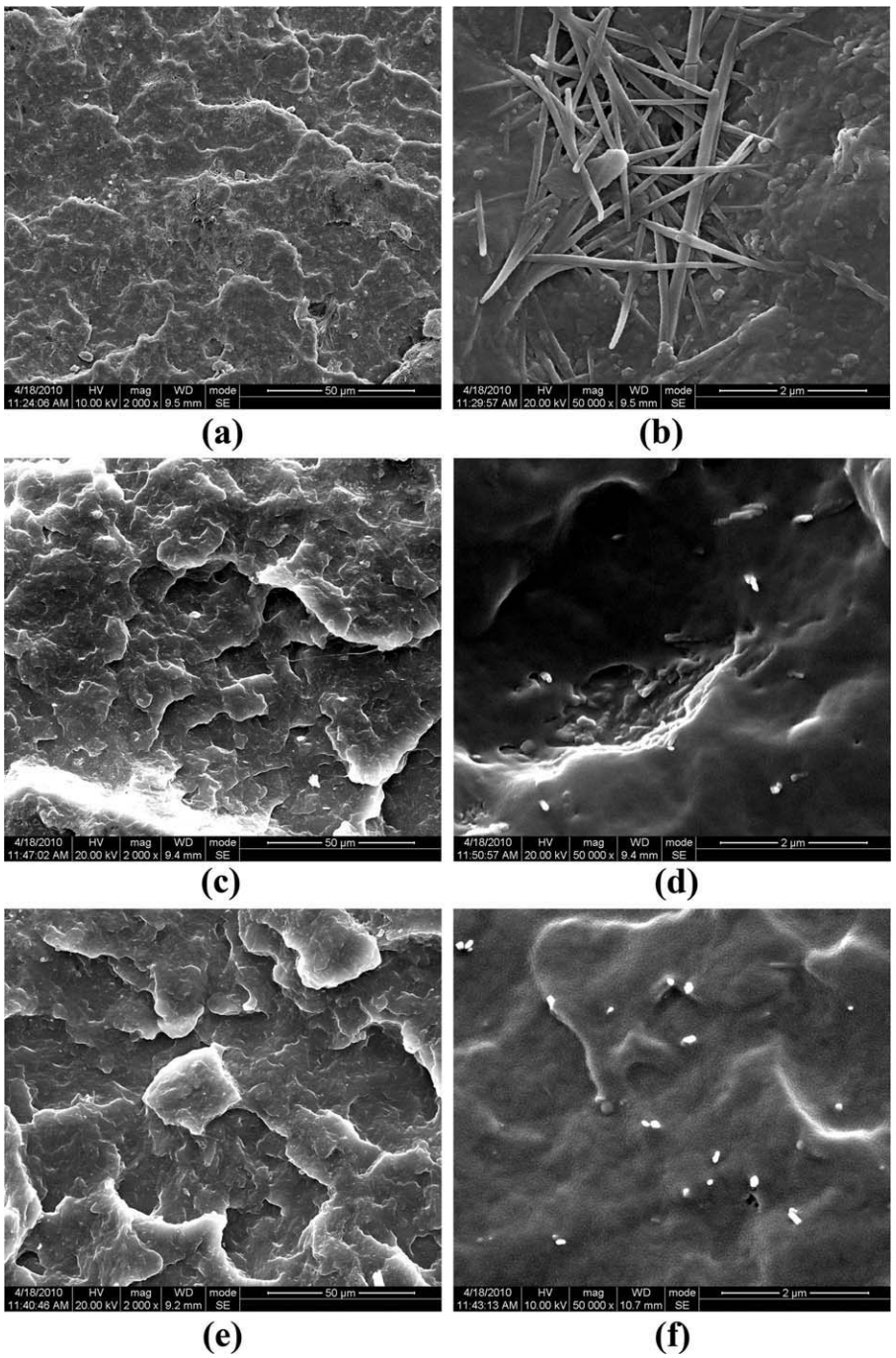

Figure 4 SEM micrographs of the impact-fractured surface of PP composites: (a,b) 2 wt % ATP, (c,d) 2 wt % ODA–ATP, and (e,f) 2 wt % ODA–aPP–ATP.

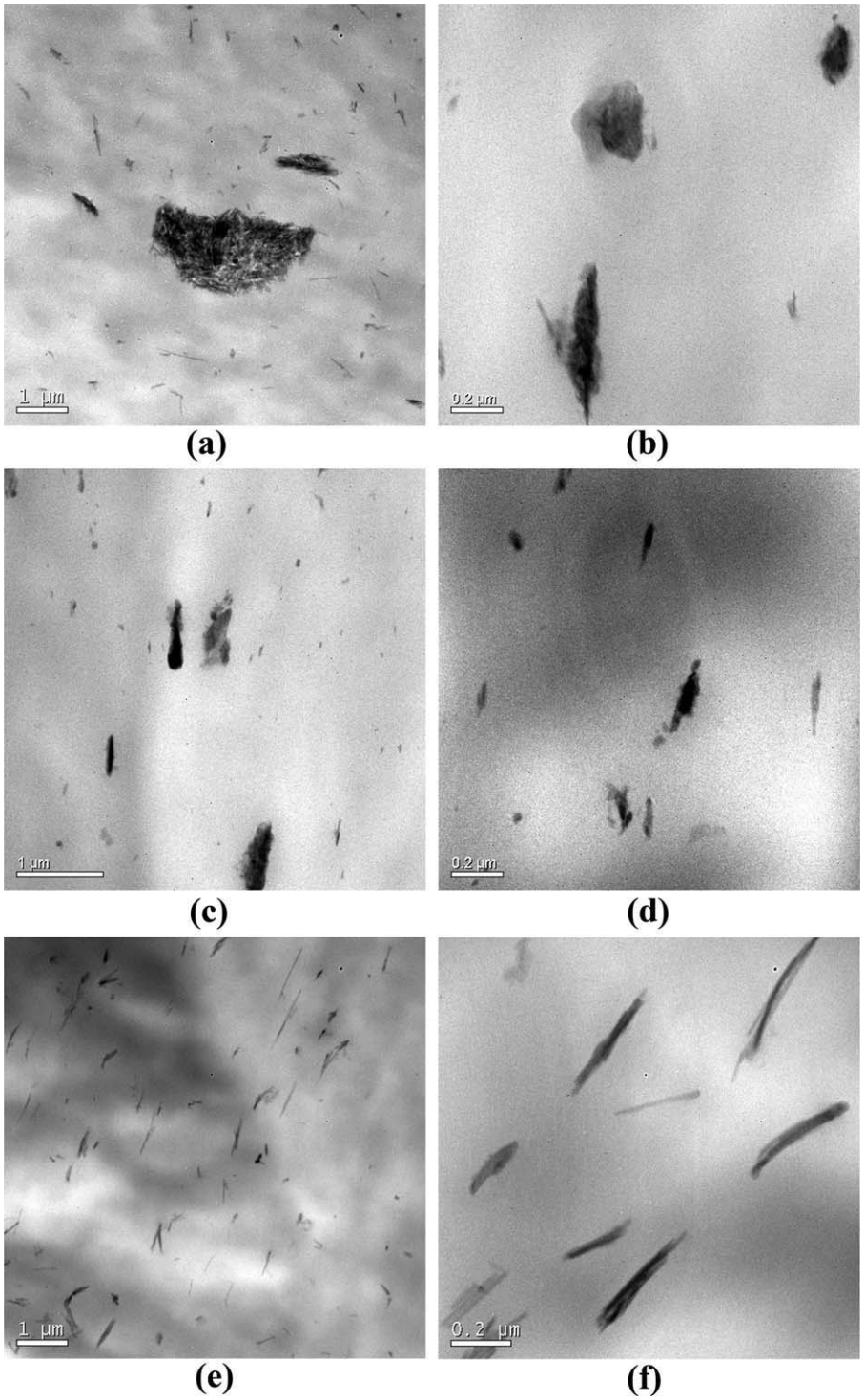

Figure 5 TEM micrographs of PP/ATP and PP/modified-ATP nanocomposites: (a,b) 2 wt % ATP, (c,d) 2 wt % ODA–ATP, and (e,f) 2 wt % ODA–aPP–ATP.

Figure 4(a) shows an SEM photo of the impact fracture surfaces of PP filled with 2 wt % original ATP and shows typical brittle fracture characteristics. Many ATP aggregates were readily observed on the fracture surface from the SEM images of the PP/2 wt % ATP specimen [Fig. 4(a,b)]. This may have contributed to the weak interaction between the original ATP and PP.

In contrast with PP/2 wt % ATP, a rougher surface appearance and more obvious plastic deformation were observed in the fractographs of the nanocomposites with 2 wt % ODA–ATP and ODA–aPP–ATP [Fig. 4(c,e)]; this proved the presence of stronger interactions between the modified ATP and PP.

The mechanical properties of rigid particles/thermoplastic composites depend not only on the

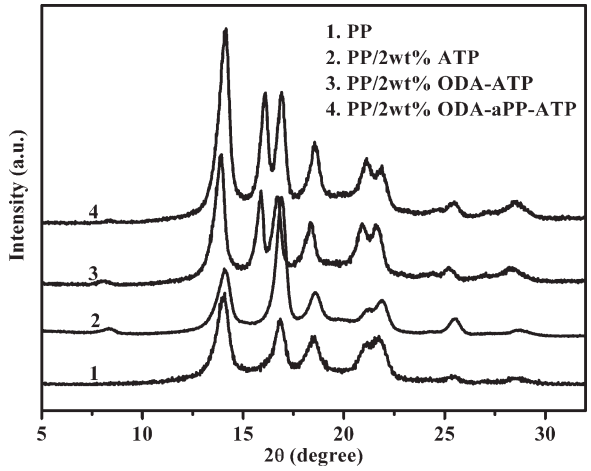

Figure 6 WAXD spectra of PP and its nanocomposites.

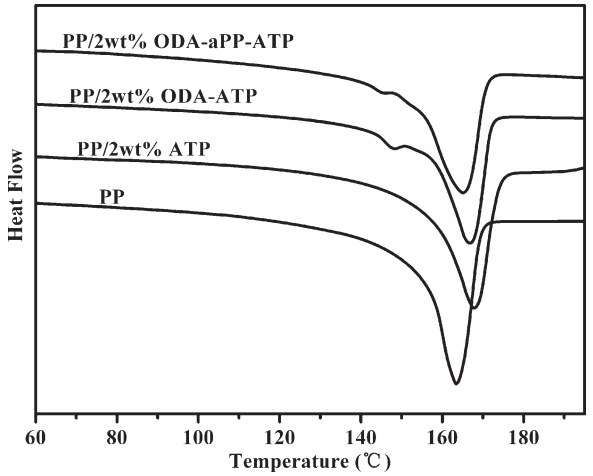

Figure 7 Melting curves of PP and its nanocomposites.

morphology of composites but also on the interfacial adhesion between the matrix and filler. An optimum particle size and good interfacial adhesion are required for effective toughening.[35] As shown in the higher magnification SEM images [Fig. 4(d,f)], some individual crystal needles were dispersed uniformly in the PP matrix, and the crystal needles were wrapped tightly by PP; this indicated that there was good interfacial adhesion between PP and the modified ATP. This effect was generally attributed to the stronger interaction between the PP matrix and modified ATP.

Dispersion of ATP in the PP nanocomposites

In general, the microscopic structure of ATP contains three levels: (1) the crystal needle as the basic structure unit, (2) a crystal bundle parallel assembled from crystal needles, and (3) a crystal cluster aggregated from crystal bundles.[36] The fibrous dispersion morphology of ATP in the PP matrix was confirmed by TEM images, as shown in Figure 5, where the bright parts are the PP matrix and the dark parts are the cross section of ATP. As shown in Figure 5(a,b), a lot of ATP aggregates were found in the PP composites filled with untreated ATP. However, most ATP aggregates were broken into primary particles 40–80 nm in diameter and 0.6–0.8 μm in length and uniformly dispersed into PP with the addition of 2 wt % ODA–ATP or ODA–aPP–ATP [Fig. 5(c–f)]. This illustrated that the surface modification of ATP promoted the homogeneous dispersion of ATP at the nanoscale. Nevertheless, a few crystal bundles were observed in the PP/2 wt % ODA–ATP nanocomposite. This may be one of the reasons that the impact strength and tensile strength of PP/2 wt % ODA–ATP were lower than those of the PP/2 wt % ODA–aPP–ATP nanocomposite.

Crystal structures of PP and its nanocomposites

The WAXD patterns of PP and its nanocomposites are shown in Figure 6. The crystallization parameters derived from the WAXD spectra are listed in Table IV. It was clear that the crystal structure of pure PP consisted of only the monoclinic α crystals of PP. For α-PP, characteristic peaks were observed at diffraction angles of $2\theta = 14.2$, 17.1, 18.6, 21.1, and 21.8°; these corresponded to the reflection planes (110), (040), (130), (111), and (041), respectively.[37] In the case of PP filled with 2 wt % of the original ATP, the same peaks were observed in the range of 2θ, which suggested that the addition of the original ATP did not affect the crystalline phase of PP. However, a new peak at about $2\theta = 16.0°$, corresponding to the (300) plane of the β form, was observed when the chemically modified ATP was added to PP.[38] This suggested that the modified ATP may have

TABLE IV
Crystal Parameters of PP and Its Nanocomposites

Sample	Crystallinity (%)	*B*	L_{110} (nm)	L_{040} (nm)	L_{130} (nm)
PP	54.19	0	12.10	13.91	10.53
PP/2 wt % ATP	52.09	0	10.35	15.05	12.39
PP/2 wt % ODA–ATP	64.09	0.1796	14.18	18.22	15.58
PP/2 wt % ODA–aPP–ATP	67.60	0.1776	13.35	17.14	15.49

L_{110}, L_{040}, L_{130} is the crystalline domain size perpendicular to the reflecting planes of 110, 040 and 130, respectively.

induced the generation of the β-crystalline phase PP, which could have led to a higher impact strength for PP.[39] To verify this assumption, the melting curves of PP and its nanocomposites were measured and are shown in Figure 7. A new melting peak of the β-crystalline phase appeared near 148°C in the differential scanning calorimetry curves of the PP/modified ATP; this clearly suggested that the modified ATP induced the formation of the β-crystalline form of PP. These results were consistent with the WAXD results.

The crystallinities of PP and its composites were obtained from the ratio between the area under the crystalline peaks and the total area under the diffraction curve, with the different contributions of the crystalline and amorphous regions considered.[40] The separation of the crystalline peaks from the amorphous halo was made in accordance with a procedure proposed by Lima et al.[41]

The relative content of the β-crystal phase was quantified by the parameter B and calculated with the following formula:[42]

$$B = \frac{I_{300}}{I_{300} + I_{110} + I_{040} + I_{130}} \quad (1)$$

where I_{300} is the intensity of the β-phase reflection, which was located at $2\theta \approx 16.0^\circ$, and I_{110}, I_{040}, and I_{130} are the intensities of the corresponding monoclinic diffraction peaks.

The average crystalline size was calculated by the Scherrer formula:[43,44]

$$L_{hkl} = \frac{0.9\lambda}{B\cos\theta} \quad (2)$$

where L_{hkl} is the crystalline domain size (nm), λ is 0.1542 nm, and θ is the diffraction angle (rad). L_{hkl} was considered as an average dimension perpendicular to the reflecting planes (*hkl*). As shown in Table IV, the crystallinity decreased slightly when the original ATP was incorporated into PP. However, the addition of modified ATP markedly increased the crystallinity of PP. The increased crystallinity may have resulted in a higher yield stress and modulus.[45] The relative content of the β-form crystal phase reached 18.0% when the modified ATP was added to PP. The average crystalline size became larger with the addition of modified ATP. This was attributed to the organic molecules at the interface between the filler and PP, which might have promoted the motion of the PP chain during crystallization.

CONCLUSIONS

aPP was chemically grafted onto ATP through the bridge linking of R303 and poly(octadecyl acrylate). When 3 wt % ODA–aPP–ATP was added to PP, the impact strength and tensile strength of PP increased by 123 and 23%, respectively, over those of pure PP. The chemically modified ATP was uniformly dispersed into PP in the form of individual crystal needles; this led to considerable enhancements in Young's modulus and the storage modulus. T_g of PP decreased evidently in the presence of the chemically grafted ATP. The crystal structure analysis revealed that the modified ATP induced the formation of the β-crystalline form of PP, and the relative content of the β-crystalline form increased to 18.0%.

References

1. Dubnikova, I. L.; Berezina, S. M.; Antonov, A. V. J Appl Polym Sci 2002, 85, 1911.
2. Denac, M.; Musil, V.; Šmit, I. Compos A 2005, 36, 1282.
3. Garcés, J. M.; Moll, D. J.; Bicerano, J.; Fibiger, R.; McLeod, D. G. Adv Mater 2000, 12, 1835.
4. Houshyar, S.; Shanks, R. A. J Appl Polym Sci 2007, 105, 390.
5. Bao, S. P.; Tjong, S. C. Compos A 2007, 38, 378.
6. Kawasumi, M.; Hasegawa, N.; Kato, M.; Usuki, A.; Okada, A. Macromolecules 1997, 30, 6333.
7. Kato, M.; Usuki, A.; Okada, A. J Appl Polym Sci 1997, 66, 1781.
8. Tjong, S. C.; Meng, Y. Z.; Hay, A. S. Chem Mater 2002, 14, 44.
9. Tarapow, J. A.; Bernal, C. R.; Alvarez, V. A. J Appl Polym Sci 2009, 111, 768.
10. Perrin-Sarazin, F.; Ton-That, M. T.; Bureau, M. N.; Denault, J. Polymer 2005, 46, 11624.
11. Song, P. A.; Tong, L. F.; Fang, Z. P. J Appl Polym Sci 2008, 110, 616.
12. Sharma, S. K.; Nema, A. K.; Nayak, S. K. J Appl Polym Sci 2010, 115, 3463.
13. Zhu, S. P.; Chen, J. Y.; Li, H. L. Polym Bull 2009, 63, 245.
14. Zhong, W. X.; Qiao, X. Y.; Sun, K.; Zhang, G. D.; Chen, X. D. J Appl Polym Sci 2006, 99, 2558.
15. Ratnayake, U. N.; Haworth, B. Polym Eng Sci 2006, 46, 1008.
16. Okada, A.; Usuki, A. Macromol Mater Eng 2006, 291, 1449.
17. Liu, H. Z.; Lim, H. T.; Ahn, K. H.; Lee, S. J. J Appl Polym Sci 2007, 104, 4024.
18. Haden, W. L.; Schwint, I. A. Ind Eng Chem 1967, 59, 58.
19. Galan, E. Clay Miner 1996, 31, 443.
20. Wang, C. H.; Auad, M. L.; Marcovich, N. E.; Nutt, S. J Appl Polym Sci 2008, 109, 2562.
21. Xue, S. Q.; Reinholdt, M.; Pinnavaia, T. J. Polymer 2006, 47, 3344.
22. Shen, L.; Lin, Y. J.; Du, Q. G.; Zhong, W.; Yang, Y. L. Polymer 2005, 46, 5758.
23. Yuan, X. P.; Li, C. C.; Guan, G. H.; Liu, X. Q.; Xiao, Y. N.; Zhang, D. J Appl Polym Sci 2007, 103, 1279.
24. Lai, S. Q.; Yue, L.; Li, T. S.; Liu, X. J.; Lv, R. G. Macromol Mater Eng 2005, 290, 195.
25. Lai, S. Q.; Yue, L.; Li, T. S. J Appl Polym Sci 2007, 106, 3091.
26. Subramani, C.; Jamnik, V. S.; Mhaske, S. T. Polym Compos 2008, 29, 890.
27. Wang, L. H.; Sheng, J. Polymer 2005, 46, 6243.
28. Zhao, L. J.; Du, Q.; Jiang, G. J.; Guo, S. Y. J Polym Sci Part B: Polym Phys 2007, 45, 2300.
29. Lei, X. P.; Liu, Y. S.; Su, Z. X. Polym Compos 2008, 29, 239.

30. Patzkó, Á.; Dékány, I. Colloid Surface A 1993, 71, 299.
31. Saule, M.; Moine, L.; Degueil-Castaing, M.; Maillard, B. Polymer 2004, 45, 5749.
32. Assoun, L.; Manning, S. C.; Moore, R. B. Polymer 1998, 39, 2571.
33. Sepe, M. P. Dynamic Mechanical Analysis for Plastics Engineering; Plastic Design Library: New York, 1998.
34. Liu, W.; Wang, Y. J.; Sun, Z. J Appl Polym Sci 2003, 88, 2904.
35. Donald, A. M.; Kramer, E. J. J Mater Sci 1982, 17, 1765.
36. Zhou, J.; Liu, L.; Li, Y.; Ma, Y. J. Bull Chin Ceram Soc 1999, 18, 50.
37. Auriemma, F.; Rosa, C. D. Macromolecules 2006, 39, 7635.
38. Luo, F.; Geng, C. Z.; Wang, K.; Deng, H.; Chen, F.; Fu, Q.; Na, B. Macromolecules 2009, 42, 9325.
39. Meng, M. R.; Dou, Q. Mater Sci Eng A 2007, 492, 177.
40. Zevin, L. S.; Kimmel, G. Quantitative X-Ray Diffractometry; Springer-Verlag: New York, 1995.
41. Lima, M.; Vasconcellos, M. Z.; Samios, D. J Polym Sci Part B: Polym Phys 2002, 40, 896.
42. Zipper, P.; Jánosi, A.; Wrentschur, E. J De Phys IV 1993, 3, 33.
43. Qu, J. P.; He, G. J.; He, H. Z.; Yu, G. H.; Liu, G. Q. Eur Polym J 2004, 40, 1849.
44. Daniel, C.; Avallone, A.; Guerra, G. Macromolecules 2006, 39, 7578.
45. van der Wal, A.; Mulder, J. J.; Gaymans, R. J. Polymer 1998, 39, 5477.